Inorganic Chemistry
Article

Inorg. Chem. **2010**, *49*, 1517–1523 **1517**
DOI: 10.1021/ic9017344

One-Dimensional Spin-Crossover Iron(II) Complexes Bridged by Intermolecular Imidazole−Pyridine NH···N Hydrogen Bonds, $[Fe(HL^{Me})_3]X_2$ (HL^{Me} = (2-Methylimidazol-4-yl-methylideneamino-2-ethylpyridine; X = PF_6, ClO_4, BF_4)

Koshiro Nishi,[†] Shinobu Arata,[†] Naohide Matsumoto,*[,†] Seiichiro Iijima,[‡] Yukinari Sunatsuki,[§] Hiroyuki Ishida,[§] and Masaaki Kojima[§]

[†]*Department of Chemistry, Faculty of Science, Kumamoto University, Kurokami 2-39-1, Kumamoto 860-8555, Japan,* [‡]*National Institute of Advanced Industrial Science and Technology, Tsukuba 305-8566, Japan, and* [§]*Department of Chemistry, Faculty of Science, Okayama University, Tsushima-naka 3-1-1, Okayama 700-8530, Japan*

Received September 1, 2009

2-Methylimidazol-4-yl-methylideneamino-2-ethylpyridine (abbreviated as HL^{Me}) is the 1:1 condensation product of 2-methyl-4-formylimidazole and 2-aminoethylpyridine and functions as a bidentate ligand to the iron(II) ion to produce the 3:1 complexes together with anions, $[Fe(HL^{Me})_3]X_2$ (X = PF_6 (**1**), ClO_4 (**2**), BF_4 (**3**)). The magnetic susceptibilities, differential scanning calorimetric measurements, and Mössbauer spectral measurements demonstrated that complexes **1**, **2**, and **3** showed a steep one-step spin crossover (SCO) between the high-spin (HS, $S = 2$) and low-spin (LS, $S = 0$) states with small thermal hysteresis. Three complexes have an isomorphous structure and are crystallized in the same monoclinic space group, *C*2/*c*, both in the HS and LS states. The iron(II) ion has the octahedral coordination geometry of a *facial* isomer with N_6 donor atoms of three bidentate ligands, in which an imidazole and an imine nitrogen atom per ligand participate in the formation of the coordination bond, but the pyridine nitrogen is free from coordination. The complex cation *fac*-$[Fe(HL^{Me})_3]^{2+}$ is a chiral species with a Δ or Λ isomer, and the adjacent Δ and Λ isomers are linked alternately by an intermolecular imidazole−pyridine NH···N hydrogen bond to produce an achiral 1D chain. The two remaining imidazole moieties per complex are hydrogen-bonded to the anions that occupy the space among the chains. The SCO profile becomes steeper with the decrease of the anion size (73.0 Å^3 for PF_6^-, 54.4 Å^3 for ClO_4^-, and 53.4 Å^3 for BF_4^-). The SCO transition temperature $T_{1/2}$ of the PF_6 (**1**), ClO_4 (**2**), and BF_4 (**3**) salts estimated from the magnetic susceptibility measurements are ($T_\downarrow$ = 151.8 K, $T_\uparrow$ = 155.3 K), ($T_\downarrow$ = 184.5 K, $T_\uparrow$ = 186.0 K), and ($T_\downarrow$ = 146.4 K, $T_\uparrow$ = 148.2 K), respectively, indicating that the $T_{1/2}$ value is not in accord with the anion size.

Introduction

Spin crossover (SCO) is a representative example of molecular bistability, in which the high-spin (HS) and low-spin (LS) states are interconvertible by physical perturbations, such as temperature, pressure, magnetic field, light, ultrashort laser, soft- and hard-X-ray radiations, and nuclear decay.[1] While SCO is described fundamentally as a phenomenon of a single molecule,[1] interesting SCO behaviors observed in the solid state, such as steep- and multistep SCO and hysteresis, have been ascribed to a cooperative effect between SCO sites.[1] From the synthetic viewpoint, to achieve a cooperative effect, polymeric SCO complexes bridged by coordination bonds[2] and mononuclear SCO complexes exhibiting intermolecular hydrogen bonding[3] or

*To whom correspondence should be addressed. Fax: +81-96-342-3390. E-mail: naohide@aster.sci.kumamoto-u.ac.jp.

(1) (a) Gütlich, P.; Goodwin, H. A. *Spin Crossover in Transition Metal Compounds I-III, Topics in Current Chemistry*; Springer: New York, 2004; pp 233−235. (b) Gütlich, P.; Garcia, Y.; Goodwin, H. A. *Chem. Soc. Rev.* **2000**, *29*, 419–427. (c) Gütlich, P.; Hauser, A.; Spiering, H. *Angew. Chem., Int. Ed. Engl.* **1994**, *33*, 2024. (d) Goodwin, H. A. *Coord. Chem. Rev.* **1976**, *18*, 293–325. (e) Gütlich, P. *Struct. Bonding* (*Berlin*) **1981**, *44*, 83. (f) König, E.; Ritter, G.; Kulshreshtha, S. K. *Chem. Rev.* **1985**, *85*, 219. (g) König, E. *Struct. Bonding* (*Berlin*) **1991**, *76*, 51. (h) Real, J. A.; Gaspar, A. B.; Niel, V.; Muñoz, M. C. *Dalton Trans.* **2005**, 2062–2079.

(2) (a) Kröber, J.; Codjovi, E.; Kahn, O.; Grolière, F.; Jay, C. *J. Am. Chem. Soc.* **1993**, *115*, 9810. (b) Real, J. A.; Gaspar, A. B.; Niel, V.; Muñoz, M. C. *Coord. Chem. Rev.* **2003**, *235*, 121. (c) Galet, A.; Muñoz, M. C.; Gaspar, A. B.; Real, J. A. *Inorg. Chem.* **2005**, *44*, 8749. (d) van Koningsbruggen, P. J.; Garcia, Y.; Codjovi, E.; Lapouyade, R.; Kahn, O.; Fournes, L.; Rabardel, L. *J. Mater. Chem.* **1997**, *7*, 2069. (e) Imatomi, S.; Sato, T.; Hashimoto, S.; Matsumoto, N. *Eur. J. Inorg. Chem.* **2009**, 721–726. (f) Ohta, S.; Yoshimura, C.; Matsumoto, N.; Okawa, H.; Ohyoshi, A. *Bull. Chem. Soc. Jpn.* **1986**, *59*, 155–159.

(3) (a) Buchen, T.; Gütlich, P.; Sugiyarto, K. H.; Goodwin, H. A. *Chem.—Eur. J.* **1996**, *2*, 1134–1138. (b) Sugiyarto, K. H.; Scudder, M. L.; Craig, D. C.; Goodwin, H. A. *Aust. J. Chem.* **2000**, *53*, 755–765. (c) Sugiyarto, K. H.; Goodwin, H. A. *Aust. J. Chem.* **1988**, *41*, 1645–1663. (d) Sunatsuki, Y.; Ikuta, Y.; Matsumoto, N.; Ohta, H.; Kojima, M.; Iijima, S.; Hayami, S.; Maeda, Y.; Kaizaki, S.; Dahan, F.; Tuchagues, J.-P. *Angew. Chem., Int. Ed.* **2003**, *42*, 1614–1618. (e) Yamada, M.; Hagiwara, H.; Torigoe, H.; Matsumoto, N.; Kojima, M.; Dahan, F.; Tuchagues, J.-P.; N. Re, N.; Iijima, S. *Chem.—Eur. J.* **2006**, *12*, 4536–4549. (f) Ikuta, Y.; Ooidemizu, M.; Yamahata, Y.; Yamada, M.; Osa, S.; Matsumoto, N.; Iijima, S.; Sunatsuki, Y.; Kojima, M.; Dahan, F.; Tuchagues, J.-P. *Inorg. Chem.* **2003**, *42*, 7001–7017. (g) Sato, T.; Iijima, S.; Kojima, M.; Matsumoto, N. *Chem. Lett.* **2009**, 178–179. (h) Sato, T.; Nishi, K.; Iijima, S.; Kojima, M.; Matsumoto, N. *Inorg. Chem.* **2009**, *48*, 7211–7229.

Published on Web 01/21/2010

$\pi-\pi$ stacking[4] have been synthesized, and interesting SCO behaviors have been discovered. On the other hand, several theoretical models have been used in order to take into account the cooperative effect in SCO transition,[5] and the origin of the cooperative nature has been investigated by considering elastic interactions among SCO molecules.[6] As the size of each molecule changes depending on its spin state, the elastic interaction among the lattice distortions provides the cooperative interaction of the spin states. However, the parameters of the theoretical model calculations are not straightforward with regard to the real molecular structure of SCO complexes. The correlation between the theoretical parameter and the structural parameter must, therefore, be established. In order to approach this problem, a series of SCO complexes exhibiting the same network structure and showing different SCO properties is helpful to understand the spin transition behavior from synthetic, structural, magnetic, and theoretical viewpoints.

In this study, we have synthesized a series of the 1:3 complexes $[Fe(HL^{Me})_3]X_2$ (X = PF_6 (**1**), ClO_4 (**2**), BF_4 (**3**)). Since they have an isomorphous one-dimensional structure constructed by intermolecular hydrogen bonds and exhibit steep one-step SCO, these are the suitable compounds by which to investigate the correlation between the structural parameters and the magnetic properties. Here, we report the syntheses, structures, and SCO properties of the iron(II) complexes. The study of the PF_6 salt has been in part reported in a previous communication.[7]

Results and Discussion

Synthesis and Characterization of $[Fe(HL^{Me})_3]X_2$ (X = PF_6 (1), ClO_4 (2), BF_4 (3)). The ligand was prepared by the 1:1 condensation reaction of 2-methyl-4-formylimidazole and 2-aminoethylpyridine in methanol. In our previous paper, the ligand was used for the synthesis of copper(II) complexes. Under acidic conditions, the protonated complex $[CuCl_2(HL^{Me})]$ was obtained, where the copper(II) ion is coordinated by a tridentate ligand (HL^{Me}) and two chloride ions. Under alkaline conditions, the perchlorate salt of the deprotonated complex $[Cu_4(L^{Me})_4](ClO_4)_4$ was obtained, where the cation has a cyclic imidazolate-bridged tetranuclear structure and the copper(II) ion is coordinated by three nitrogen atoms of a tridentate ligand, HL^{Me}, and one imidazolate nitrogen atom of the adjacent copper(II) unit.[8] In the case of the iron(II) complexes, the ligand can function as either a bidentate or tridentate ligand to produce the 3:1 $[Fe(HL^{Me})_3]^{2+}$ or 2:1 $[Fe(HL^{Me})_2]^{2+}$ complexes, respectively. The 2:1 complex $[Fe(HL^{Me})_2](PF_6)_2$ and the 3:1 complex $[Fe(HL^{Me})_3](PF_6)_2$ were prepared by mixing the ligand, $FeCl_2 \cdot 4H_2O$, and KPF_6 in 2:1:2 and 3:1:2 molar ratios, respectively.[7] In this study, the ClO_4 and BF_4 salts of the 1:3 complexes were prepared by a similar way to that for the PF_6 salt, using $NaClO_4$ and $NaBF_4$ instead of KPF_6. Well-grown crystals of these iron(II) complexes (5 mm or larger in dimension) can be obtained from slow crystallization and evaporation of the solvent at room temperature in the air. The Mössbauer spectrum of the PF_6 salt indicated the existence of impurity due to high-spin Fe^{III} species, suggesting that the synthesis in an inert atmosphere is preferable. The formula of $[Fe(HL^{Me})_3]X_2$ was confirmed by elemental analyses and crystal structure analyses, suggesting no crystal solvents. The existence of the crystal solvent for the BF_4 and PF_6 salts was further examined by TGA (thermogarvimetric analysis), while the measurement of the ClO_4 salt was not performed due to potential explosion. The samples were heated from room temperature to 130 °C. No decrease of the sample weight for the BF_4 salt is observed, and a 0.3% weight loss corresponding to a molecular weight of ca. 3 for the PF_6 salt was observed. These complexes showed a thermochromism in the solid states from yellow at ambient temperature to dark red at liquid nitrogen temperature, suggesting a SCO.

Magnetic Properties of $[Fe(HL^{Me})_3]X_2$ (X = PF_6 (1), ClO_4 (2), BF_4 (3)). The magnetic susceptibility was measured upon cooling from 300 to 5 K and then measured upon warming from 5 to 300 at a 0.5 K min^{-1} rate under a 0.5 T applied magnetic field by the use of a SQUID magnetometer. The $\chi_M T$ versus T plots for the ground samples of three complexes are shown in Figure 1, demonstrating a complete one-step, steep SCO between HS ($S = 2$) and LS ($S = 0$) states. In the higher-temperature region, the constant $\chi_M T$ value of ca. 3.3 cm^3 K mol^{-1} is compatible with the reported HS Fe^{II} ($S = 2$) complexes. In the lower-temperature region, a plateau value of nearly 0 cm^3 K mol^{-1} is compatible with the expected value for LS Fe^{II} ($S = 0$) complexes. In the region of the spin-transition temperature, the $\chi_M T$ value changes steeply between the HS and LS values with small thermal hysteresis. The steepness of the SCO transition is in the order of $PF_6 < ClO_4 < BF_4$. The SCO transition temperature, $T_{1/2}$, of the PF_6 (**1**), ClO_4 (**2**), and BF_4 (**3**) salts are $T_\downarrow$ = 151.8 K, $T_\uparrow$ = 155.3 K; $T_\downarrow$ = 184.5 K, $T_\uparrow$ = 186.0 K; and $T_\downarrow$ = 146.4 K, $T_\uparrow$ = 148.2 K, respectively. As the counteranions used in this study can be described as isotropic molecules, the molecular volumes can be evaluated by quantum-chemical calculations to be 53.4 $Å^3$ for BF_4^-, 54.4 $Å^3$ for ClO_4^-, and 73.0 $Å^3$ for PF_6^-, respectively.[3e,9] The spin transition, therefore, becomes steeper with the decrease of the size of the counteranion, while the $T_{1/2}$ values are not in accord with the order of the anion size.

DSC Measurements. The differential scanning calorimetry (DSC) measurements were carried out in the 128−250 K temperature range, at a 5 K min^{-1} sweeping rate, where in the temperature region of the SCO transition, the ClO_4 (**2**) and BF_4 (**3**) salts showed a sharp peak, but the PF_6 salt showed a broad peak. The DSC curves of the BF_4 salt (**3**) are shown in Figure 2. The transition temperatures have been determined to be ca. 154 and 153 K

(4) (a) Hayami, S.; Gu, Z.; Shiro, M.; Einaga, Y.; Fujishima, A.; Sato, O. *J. Am. Chem. Soc.* **2000**, *122*, 7126. (b) Hayami, S.; Hiki, K.; Maeda, Y.; Urakami, D.; Inoue, K.; Ohama, M.; Kawata, S.; Sato, O. *Chem.—Eur. J.* **2009**, *15*, 3497–3508. (c) Hagiwara, H.; Hashimoto, S.; Matsumoto, N.; Iijima, S. *Inorg. Chem.* **2007**, *46*, 3136–3143.

(5) (a) Slichter, C. P.; Drickamer, H. G. *J. Chem. Phys.* **1972**, *56*, 2142. (b) Sorai, M.; Seki, S. *J. Phys. Chem. Solids* **1974**, *35*, 555. (c) Wajnflasz, J.; Pick, R. *J. Phys.* (*Paris*) **1971**, *32*, C1−91. (d) Bosseksou, A.; Varret, F.; Nasser, J. *J. Phys.* (*Paris*) **1993**, *I3*, 1463. (e) Nishino, M.; Bouheddaden, K.; Miyashita, S.; Varret, F. *Phys. Rev. B* **2003**, *68*, 224402.

(6) (a) Nishino, M.; Bouheddaden, K.; Konishi, Y.; Miyashita, S. *Phys. Rev. Lett.* **2007**, *98*, 247203. (b) Konishi, Y.; Tokoro, H.; Nishino, M.; Miyashita, S. *Phys. Rev. Lett.* **2008**, *100*, 067206. (c) Miyashita, S.; Konishi, Y.; Nishino, M.; Tokoro, H.; Rikvold, P. A. *Phys. Rev. B* **2008**, *77*, 014105.

(7) Arata, S.; Hamamatsu, T.; Sato, T.; Iihoshi, T.; Matsumoto, N.; Iijima, S. *Chem. Lett.* **2007**, 778–779.

(8) (a) Matsumoto, N.; Motoda, Y.; Matsuo, T.; Nakashima, T.; Re, N.; Dahan, F.; Tuchagues, J.-P. *Inorg. Chem.* **1999**, *38*, 1165–1173. (b) Sunatsuki, Y.; Motoda, Y.; Matsumoto, N. *Coord. Chem. Rev.* **2002**, *226*, 199–209.

(9) *Spartan*, version 4.0; Wavefunction, Inc.: Irvine, CA, 1999.

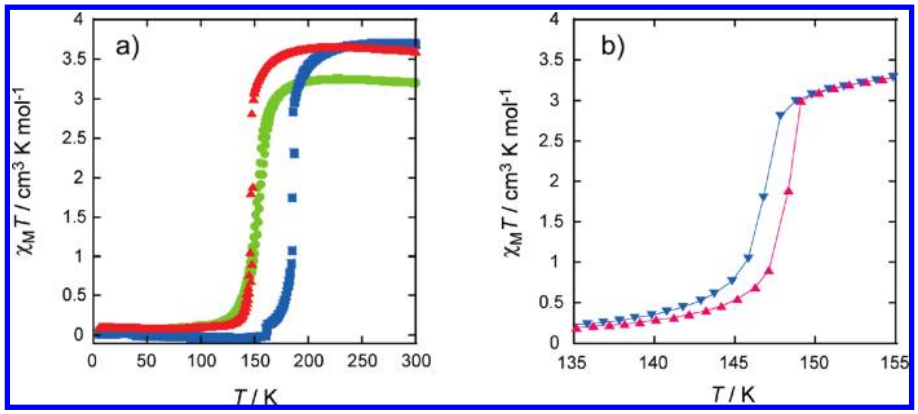

Figure 1. (a) One-step, steep SCO behaviors of $[Fe(HL^{Me})_3]X_2$ (X = PF_6 (green circle), ClO_4 (blue square), BF_4 (red triangle), in the form of $\chi_M T$ versus T plots, where the values $\chi_M T$ are plotted between 300 and 5 at a 0.5 K min^{-1} rate under a 0.5 T applied magnetic field. The $\chi_M T$ value was measured upon cooling from 300 to 5 K, and then upon warming from 5 to 300 K. (b) Hysteresis loop of the BF_4 salt (**3**) with $T_\downarrow$ = 146.4 K and $T_\uparrow$ = 148.2 K in the plots of $\chi_M T$ versus T. The warming and cooling modes are plotted by red- and blue-colored triangles, respectively.

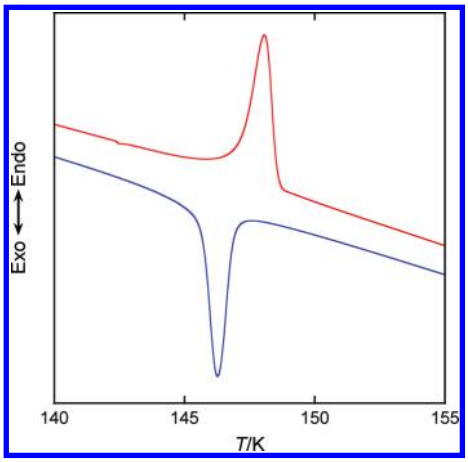

Figure 2. Differential scanning calorimetry (DSC) curves in the spin-crossover region for the BF_4 salt (**3**).

for the PF_6 salt (**1**), ca. 186 and 184 K for the ClO_4 salt (**2**), and ca. 148 and 146 K for the BF_4 salt (**3**), in the heating and cooling modes, respectively. These values agree well with those observed in the $\chi_M T$ versus T plot. The enthalpy (ΔH) and entropy (ΔS) variations can be estimated for the ClO_4 (**2**) and BF_4 (**3**) salts. The value of the heating and cooling modes are ΔH = 7.1 kJ mol^{-1} and ΔS = 38 J K^{-1} mol^{-1} for the ClO_4 salt and ΔH = 5.3 kJ mol^{-1} and ΔS = 36 J K^{-1} mol^{-1} for the BF_4 salt. The estimated entropy variations are much larger than the entropy gain R ln 5 = 13.4 J mol^{-1} K^{-1} due to the $S = 0 \rightarrow S = 2$ change in spin-only value for iron(II) SCO systems.

The temperature dependence of the Mössbauer spectra of $[Fe(HL^{Me})_3](PF_6)_2$ (**1**) was investigated in the temperature range of 78−240 K. Representative spectra in the warming mode are shown in Figure 3a. At 78 K in the LS state, the spectrum consists only of a doublet assignable to LS Fe^{II} (isomer shift δ = 0.50 mm s^{-1} and quadruple splitting ΔE_Q = 0.22 mm s^{-1}). At the SCO temperature region of 150−170 K, the spectrum consists of two doublets assignable to the LS and HS Fe^{II} species (for example, at 160 K, LS Fe^{II} (δ = 0.48 mm s^{-1}, ΔE_Q = 0.23 mm s^{-1}) and HS Fe^{II} (δ = 1.08 mm s^{-1}, ΔE_Q = 1.26 mm s^{-1})). At 200 K in the HS state, the spectrum consists of a doublet assignable to HS Fe^{II} species (δ = 1.07 mm s^{-1} ΔE_Q = 1.10 mm s^{-1}) and signals of an unidentified impurity, probably due to Fe^{III} species. The unidentified component is attributable to a HS Fe^{III} species, such as Fe^{III} oxide fine particles, which have a small quadrupole splitting and an isomer shift ranging from 0.3 to 0.4 mm s^{-1}.[10] Because the Debye temperature of the impurity Fe^{III} is far higher than that of Fe^{II} in complex **1**, the absorption of the impurity becomes apparent at higher temperatures[11] and the relative value of the impurity looks very high, but the real percentage of the impurity is equal to the value evaluated from the low-temperature spectrum. The spectrum at 78 K consists only of a doublet assignable to LS Fe^{II}, which means the content of the impurity Fe^{III} is fairly low. As shown in Figure 3b, the Mössbauer results are consistent with the result from the magnetic susceptibility measurements.

Crystal Structures of $[Fe(HL^{Me})_3]X_2$ (X = PF_6 (1), ClO_4 (2), BF_4 (3)). The crystal structures of $[Fe(HL^{Me})_3]X_2$ (X = PF_6 (**1**), ClO_4 (**2**), BF_4 (**3**)) were determined in the HS and LS Fe^{II} states by the single-crystal X-ray diffraction analyses. Table 1 shows the crystallographic data of these complexes in the HS and LS states, demonstrating that these complexes assume an isomorphous structure in the HS and LS states, where the same atom numbering scheme except for the anion is taken throughout the complexes as well as their spin states. The crystal system and the space group $C2/c$ do not change during the spin transition. The unit cell shows the volume reduction of 4.1, 5.0, and 5.0% during the HS → LS spin transition for the PF_6, ClO_4, and BF_4 salts, respectively, whose values are in the reported values. Table 2 summarizes the relevant bond distances and angles, as well as the intermolecular hydrogen-bond distances. The crystallographic unique unit consists of one complex cation of $[Fe(HL^{Me})_3]^{2+}$ and two counteranions. It should be noted that, among the three salts and two spin states, the counteranions BF_4^- in the HS state are subjected to disorder. The crystal structures of $[Fe(HL^{Me})_3](ClO_4)_2$ (**2**) in the HS and LS states are exemplified in detail. Figure 4 shows the molecular structure of the complex cation in the

(10) (a) Cannas, C.; Concas, G.; Musinu, A.; Piccaluga, G.; Spano, G. *Z. Naturforsch.* **1999**, *54a*, 513. (b) Rancourt, D. G.; Daniels, J. M.; Nazar, L. F.; Gozin, G. A. *Hyperfine Interact.* **1983**, *15/16*, 653.

(11) (a) Kitazawa, T.; Gomi, Y.; Akahashi, M.; Takeda, M.; Enomoto, M.; Miyazaki, A.; Enoki, T. *J. Mater. Chem.* **1996**, *6*, 119. (b) Kunkeler, P. J.; van Koningsbruggen, P. J.; Cornelissen, J. P.; van der Horst, A. N.; van der Kraan, A. M.; Spek, A. L.; Haasnoot, J. G.; Reedijk, J. *J. Am. Chem. Soc.* **1996**, *118*, 2190.

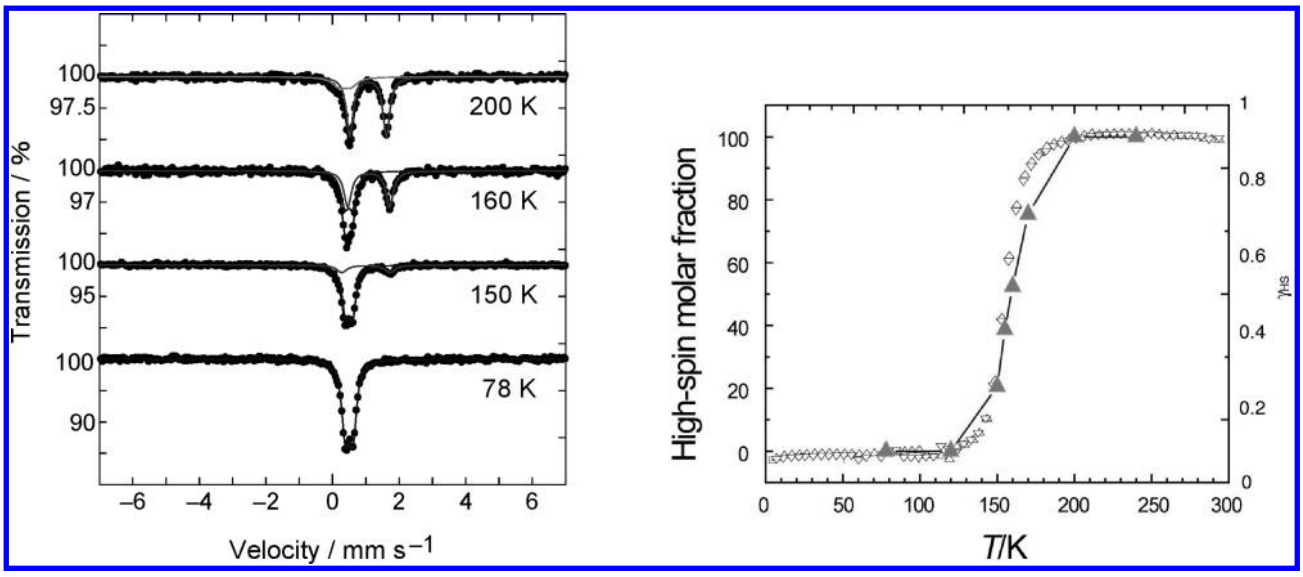

Figure 3. (a) Selected ^{57}Fe Mössbauer spectra of $[Fe(HL^{Me})_3](PF_6)_2$ (**1**) recorded at 78, 150, 160, and 200 K upon warming the sample. The HS and LS signals are derived from the deconvolution analyses. (b) Molar fraction of HS versus total Fe^{II} for $[Fe^{II}(HL^{Me})_3](PF_6)_2$ (**1**) obtained by deconvolution analysis of the Mössbauer spectra (▲), together with n_{HS} obtained by magnetic susceptibility measurements. The value of n_{HS} was calculated by using the equation $(\chi_M T)_{obs} = n_{HS}(\chi_M T)_{HS} + (1 - n_{HS})(\chi_M T)_{LS}$, with $(\chi_M T)_{HS} = 3.3$ cm^3 K mol^{-1} and $(\chi_M T)_{LS} = 0.0$ cm^3 K mol^{-1} as limiting values.

Table 1. X-Ray Crystallographic Data for $[Fe(HL^{Me})_3]X_2$ (X = PF_6 (**1**), ClO_4 (**2**), BF_4 (**3**)) in the HS and LS States

	PF_6		ClO_4		BF_4	
	200 K	123 K	250 K	150 K	250 K	150 K
formula	$C_{36}H_{42}FeN_{12}P_2F_{12}$	$C_{36}H_{42}FeN_{12}P_2F_{12}$	$C_{36}H_{42}FeN_{12}Cl_2O_8$	$C_{36}H_{42}FeN_{12}Cl_2O_8$	$C_{36}H_{42}FeN_{12}B_2F_8$	$C_{36}H_{42}FeN_{12}B_2F_8$
fw	988.58	988.58	897.56	897.56	872.26	872.26
cryst syst	monoclinic	monoclinic	monoclinic	monoclinic	monoclinic	monoclinic
space group	*C*2/*c* (No. 15)	*C*2/*c* (No. 15)	*C*2/*c* (No. 15)	*C*2/*c* (No. 15)	*C*2/*c* (No. 15)	*C*2/*c* (No. 15)
a, Å	37.408(7)	37.02(1)	37.523(11)	36.369(11)	37.478(10)	36.343(14)
b, Å	11.474(3)	11.057(3)	11.226(2)	11.294(4)	11.143(4)	11.227(5)
c, Å	22.196(4)	22.573(6)	21.604(7)	21.224(6)	21.581(5)	21.079(8)
β, deg	114.665(7)	116.075(9)	114.177(13)	115.243(11)	114.523(8)	115.172(11)
V, Å^3	8657(2)	8299(3)	8302(4)	7886(4)	8199(4)	7784.2(6)
Z	8	8	8	8	8	8
D_{calcd}, Mg m^{-3}	1.517	1.582	1.436	1.512	1.413	1.488
μ(Mo Kα), mm^{-1}	0.517	0.540	0.557	0.586	0.448	0.471
R	0.050	0.052	0.058	0.049	0.109	0.075
wR	0.146	0.141	0.177	0.136	0.295	0.190

LS state, together with the selected atom numbering schemes. The cation $[Fe(HL^{Me})_3]^{2+}$ and two anions ClO_4^- showed no disorder in both the HS and LS structures. The Fe^{II} ion is coordinated octahedrally by N_6 donor atoms of three bidentate ligands HL^{Me}, in which one imidazole and one imine nitrogen atom per ligand participate in the coordination, but the pyridine nitrogen of the 2-iminoethylpyridine moiety is free from coordination. Of two possible geometric *fac* and *mer* isomers, the complex assumes the fac isomer. The complex is a chiral species with the Δ or Λ isomer due to clockwise and counterclockwise arrangements of three bidentate ligands around the iron(II) ion. Since the space group *C*2/*c* is a centrosymmetric space group, the crystal structure consists of Δ-*fac*-$[Fe(HL^{Me})_3]^{2+}$ and Λ-*fac*-$[Fe(HL^{Me})_3]^{2+}$ isomers.

On the basis of the Fe−N bond distances and N−Fe−N bond angles, the spin state can be identified. At 250 K, the Fe−N distances are in the range of 2.171(2)−2.231(3) Å, typical for HS Fe^{II} bound to N_6 donors. At 150 K, the Fe−N distances are in the range of 1.985(2)−2.006(2) Å, typical for LS Fe^{II}. The average Fe−N distance decreases from 2.190 Å at 250 K to 1.998 Å at 150 K by 0.19 Å, which is comparable with the value of the previously reported SCO complexes (ca. 0.2 Å). The N−Fe−N bond angles also indicate the spin state of the Fe^{II} ion. For example, a bite angle of bidentate chelate N(2)−Fe−N(3) is 77.2° at 250 K and 81.6° at 150 K, and the angle of N(2)−Fe−N(7) is 171.1° at 250 K and 174.6° at 150 K. As given in Table 2, the coordination bond angles in the LS state at 150 K are closer to a regular octahedron than those in the HS state at 250 K.

The crystal packing diagram of the ClO_4 salt at 250 K is shown in Figure 5. The most striking structural feature is a one-dimensional (1D) chain structure constructed by the intermolecular NH···N hydrogen bond between an imidazole group of a cationic complex, N(1)−H, and a pyridine nitrogen of the adjacent molecule, N(8), where the hydrogen bond distance of N(1)···N(8) is 2.893(5) and 2.859(4) Å at 250 and 150 K, respectively. One of three imidazole groups per complex molecule participates in the construction of the 1D chain structure, and the remaining two imidazole groups are hydrogen-bonded to the two ClO_4^- ions with hydrogen bond distances of N(5)···O(8) = 2.866(5) and N(9)···O(4) = 2.839(5) Å

Table 2. Selected Bond Lengths (Å), Angles (deg), and Hydrogen-Bond Distances (Å) for $[Fe(HL^{Me})_3]X_2$ (X = PF_6 (**1**), ClO_4 (**2**), BF_4 (**3**)) in the HS and LS States

	PF_6		ClO_4		BF_4	
	200 K	123 K	250 K	150 K	250 K	150 K
Fe(1)−N(2)	2.183(2)	1.999(3)	2.172(3)	2.003 (2)	2.179(6)	2.014(5)
Fe(1)−N(3)	2.177(2)	1.994(2)	2.192(2)	1.992(2)	2.194(5)	2.000(4)
Fe(1)−N(6)	2.159(2)	2.007(2)	2.177(2)	2.007(2)	2.179(5)	1.998(4)
Fe(1)−N(7)	2.246(3)	2.005(3)	2.231(3)	2.006(2)	2.228(6)	1.999(5)
Fe(1)−N(10)	2.168(2)	1.991(2)	2.171(2)	1.994(2)	2.173(5)	1.998(4)
Fe(1)−N(11)	2.203(2)	1.990(2)	2.199(2)	1.985(2)	2.206(5)	1.989(4)
average Fe−N	2.189	1.998	2.190	1.999	2.193	2.000
N(2)−Fe(1)−N(3)	77.38(9)	81.2(1)	77.26(12)	81.64(9)	77.0(2)	81.4(2)
N(2)−Fe(1)−N(6)	96.60(9)	94.8(1)	95.58(11)	94.59(9)	95.1(2)	95.0(2)
N(2)−Fe(1)−N(7)	172.60(7)	175.53(9)	171.14(9)	174.60(7)	170.07(18)	174.44(16)
N(2)−Fe(1)−N(10)	92.86(9)	93.3(1)	93.78(11)	92.61(9)	94.3(2)	92.9(2)
N(2)−Fe(1)−N(11)	94.04(9)	90.8(1)	93.97(11)	89.30(9)	95.1(2)	89.3(2)
N(3)−Fe(1)−N(6)	92.10(8)	89.64(9)	91.00(9)	90.42(8)	91.6(2)	90.57(18)
N(3)−Fe(1)−N(7)	98.55(9)	97.0(1)	97.03(11)	94.51(9)	96.7(2)	94.6(2)
N(3)−Fe(1)−N(10)	168.58(9)	173.1(1)	169.57(11)	173.13(9)	170.1(2)	173.1(2)
N(3)−Fe(1)−N(11)	97.31(8)	94.5(1)	97.54(10)	94.41(8)	98.5(2)	94.62(19)
N(6)−Fe(1)−N(7)	77.25(9)	81.1(1)	77.59(11)	81.61(9)	77.3(2)	81.2(2)
N(6)−Fe(1)−N(10)	94.94(8)	95.1(1)	95.23(10)	93.80(8)	93.9(2)	93.67(19)
N(6)−Fe(1)−N(11)	167.11(8)	173.53(9)	168.39(9)	174.19(7)	167.10(19)	173.75(17)
N(7)−Fe(1)−N(10)	91.78(8)	88.8(1)	92.48(11)	91.47(9)	92.5(2)	91.4(2)
N(7)−Fe(1)−N(11)	92.60(9)	93.4(1)	93.50(11)	94.78(9)	93.5(2)	94.9(2)
N(10)−Fe(1)−N(11)	77.25(9)	81.3(1)	77.54(10)	81.70(8)	77.3(2)	81.51(19)
N(1)···N(8)*	2.921(4)	2.876(4)	2.893(5)	2.859(4)	2.903(10)	2.873(8)
N(5)···F(8) or O(8)	3.013(4)	3.047(4)	3.013(4)	3.047(4)	3.013(4)	2.788(6)
N(9)···F(5) or O(4)	2.907(3)	3.001(4)	3.233(4)	3.092(3)	3.233(4)	3.092(3)

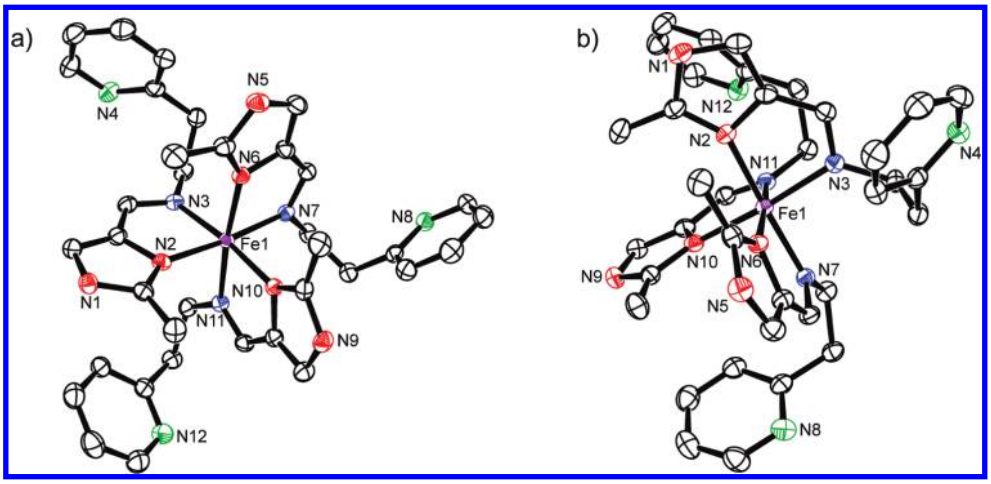

Figure 4. ORTEP drawings of a complex-cation *fac*-$[Fe(HL^{2\text{-}Me})_3]^{2+}$ of $[Fe(HL^{2\text{-}Me})_3](ClO_4)_2$ (**2**) in the LS state at 150 K with 50% thermal probability ellipsoids and selected atom numbering scheme. The hydrogen atoms are omitted for clarity. The imidazole, imine, and pyridine nitrogen atoms are drawn by red-, blue-, and green-colored ink, respectively. Due to the clockwise and anticlockwise arrangements of three bidentate ligands around iron(II) ion of *fac*-$[Fe(HL^{2\text{-}Me})_3]^{2+}$, the complex is a chiral molecule with Δ- or Λ-isomer. (**a**) *fac*-$[Fe(HL^{2\text{-}Me})_3]^{2+}$ is viewed along the pseudo C_3 axis. (**b**) Side view of *fac*-$[Fe(HL^{2\text{-}Me})_3]^{2+}$.

at 250 K. Within a chain, Δ-*fac*-$[Fe(HL^{Me})_3]^{2+}$ and Λ-*fac*-$[Fe(HL^{Me})_3]^{2+}$ isomers are linked alternately by the hydrogen bond to produce an achiral 1D chain. As shown in Figure 5a and b, the anions are hydrogen-bonded to the 1D chain but do not contribute to the formation of the 1D chain. Further, the anions show no interchain interaction, at least by hydrogen bond. Although there are no interchain hydrogen bonds, the adjacent 1D chains, including the anions, are stacked so as to compensate and adjust their undulated shapes of the chains. The TGA measurements indicated a lack of solvent of crystallization, and the result is consistent with this crystal packing of 1D chains, as shown in Figure 6. We can, therefore, expect easily that the anions can affect the cooperativity due to the molecular volume change of the spin-transition molecules both in the intra- and inter-chain interactions.

Correlation between SCO Property and Anion Size. It is difficult to correlate structure and function in spin-transition materials. The studies of isostructural SCO materials are, therefore, an important first step in learning the mechanism of the SCO. However, few such studies have been available up to now. The study on $[Fe(NCS)_2(PM\text{-}X)_2]$ compounds by Guionneau et al. is the most extensive structure−function study.[12] The present complexes

(12) (a) Guionneau, P.; Letrad, J.-F.; Yufit, D. S.; Chasseau, D.; Bravic, G.; Goeta, A. E.; Howard, J. A. K.; Kahn, O. *J. Mater. Chem.* **1999**, *9*, 985–994. (b) Guionneau, P.; Marchivie, M.; Bravic, G.; Letrad, J.-F.; Chasseau, D. Topics in Current Chemistry. *Spin Crossover in Transition Metal Compounds II*; Gütlich, P., Goodwin, H. A, Eds.; Springer: New York, 2004; Vol. *234*, pp 97−128.

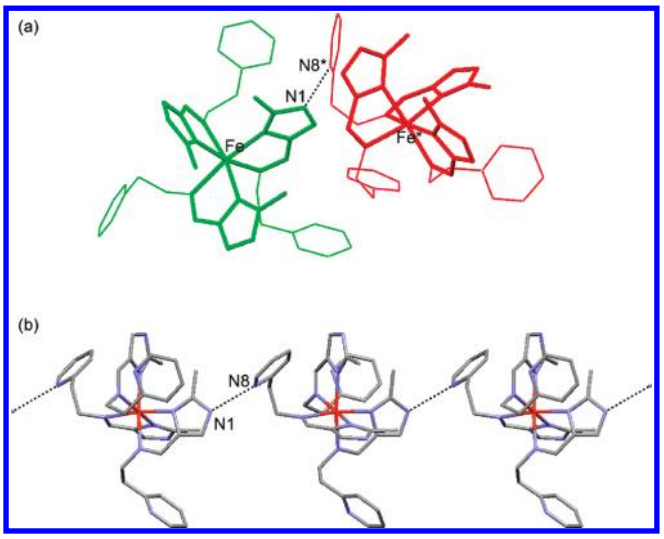

Figure 5. (a) Δ and Λ isomers of *fac*-$[Fe(HL^{Me})_3]^{2+}$ species connected alternately by the intermolecular NH···N hydrogen bond between an imidazole group of a cationic complex N(1)−H and a pyridine nitrogen of the adjacent molecule N(8). Two adjacent iron(II) complexes drawn in green and red colors are related by a symmetry operation of the *c*-glide plane. (b) 1D structure of $[Fe(HL^{Me})_3](ClO_4)_2$ (**2**) constructed with the intermolecular NH···N hydrogen bond. The remaining two imidazole groups per unit are hydrogen-bonded to two ClO_4 anions.

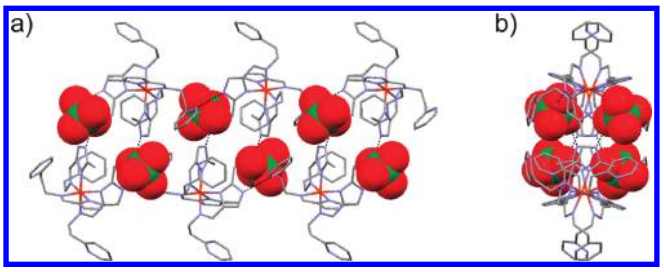

Figure 6. (a) Stacking manner of the adjacent chains of **2**. The adjacent 1D chains, including the anions, are stacked so as to compensate and adjust their undulated shapes of the chains, where the anions are drawn with the space filling model. (b) Side view of the stacking manner of the adjacent two chains, showing that the anions occupy the space between the 1D chains.

$[Fe(HL^{Me})_3]X_2$ (X = PF_6 (**1**), ClO_4 (**2**), BF_4 (**3**)) give another such example, because they have an isomorphous structure for the series and in the HS and LS states. The crystal structures assume a 1D chain constructed by an intermolecular imidazole−pyridine hydrogen bond. The anions are involved in the 1D chain via the hydrogen bonds, but there is no interchain hydrogen bond network. It can be described that the adjacent 1D chains are arrayed along the *c* axis and the anions occupy the spaces among the chains. A steep SCO of the complexes can be rationalized by the 1D structure constructed by the intermolecular imidazole−pyridine hydrogen bonds. The steepness is in the order of PF_6 (**1**) < ClO_4 (**2**) < BF_4 (**3**). The molecular volumes are 53.4 Å^3 for BF_4^-, 54.4 Å^3 for ClO_4^-, and 73.0 Å^3 for PF_6^-, respectively.[3e,9] The results demonstrate that the spin transition becomes steeper with the decrease of the size of the counteranion. This tendency is in accord with the results of $[Fe(pic)_3]X_2$ (pic = 2-picolylamine, X = Cl, Br, I), where the influence of the anion was examined, and the degree of completion and steepness of the spin transition curve increases in the order of iodide < bromide < chloride.[13] Our present results and those for $[Fe(pic)_3]X_2$ (X = Cl, Br, I) are in accord with the elastic origin of the cooperative nature of SCO. As the size of each molecule changes depending on its spin state, the elastic interaction among the lattice distortions provides the cooperative interaction of the spin states, and the cooperative interaction is more effective in the case of smaller counteranions.

The SCO transition temperature $T_{1/2}$ of the PF_6 (**1**), ClO_4 (**2**), and BF_4 (**3**) salts are estimated from the magnetic measurements to be $T_\downarrow$ = 151.8 K, $T_\uparrow$ = 155.3 K; $T_\downarrow$ = 184.5 K, $T_\uparrow$ = 186.0 K; and $T_\downarrow$ = 146.4 K, $T_\uparrow$ = 148.2 K, respectively, and the result is not in the order of the anion size. This can be examined by the DSC measurements. The Gibbs free energy ΔG accompanying the transformation from LS to HS is $\Delta G = \Delta H - T\Delta S$, where $\Delta G = G_{HS} - G_{LS}$, $\Delta H = H_{HS} - H_{LS}$, and $\Delta S = S_{HS} - S_{LS}$. The same number of HS and LS molecules is defined by $\Delta G = 0$. Hence, at the $\Delta G = 0$, we can get $T_{1/2} = \Delta H/\Delta S$. From the DSC measurements, the values of ΔH = 7.1 kJ mol^{-1} and ΔS = 38 J K^{-1} mol^{-1} for ClO_4 (**2**) and ΔH = 5.3 kJ mol^{-1} and ΔS = 36 J K^{-1} mol^{-1} for BF_4 (**3**) were evaluated. The entropy variation ΔS may be written as the sum of electronic ΔS_{el}, vibrational ΔS_{vib}, and order/disorder contribution $\Delta S_{disorder}$. The ΔS values of two complexes are similar to each other, suggesting that there is no significant difference between the ΔS values of two complexes. Rather, the value ΔH showed a significant difference and contributed to determine the transition temperature. At present, we could not find out the reason for the exceptional tendency of the transition temperatures for the series of the complexes.

Concluding Remarks

It is difficult to predict the correlation between the SCO parameters and structural parameters, because it has been well-known that the SCO properties are affected complexly by many subfactors. In this study, a series of 1:3 complexes, $[Fe(HL^{Me})_3]X_2$ (X = PF_6 (**1**), ClO_4 (**2**), BF_4 (**3**)), have been synthesized, and the SCO properties have been investigated. They have an isomorphous one-dimensional structure constructed by an intermolecular hydrogen bond, where the adjacent complex cations $[Fe(HL^{Me})_3]^{2+}$ are linked by intermolecular imidazole−pyridine NH···N hydrogen bond to produce an achiral 1D chain, and the remaining two imidazole moieties per complex are hydrogen-bonded to the anions which just occupy the space among the chains. These are, therefore, suitable compounds by which to investigate the correlation between the structural parameters and the magnetic properties: (1) The SCO profile becomes steeper with the decrease of the anion size (73.0 Å^3 for PF_6^-, 54.4 Å^3 for ClO_4^-, 53.4 Å^3 for BF_4^-). This tendency is rationalized by the fact that the positive effective cooperativity is achieved by smaller-size anions within a 1D chain. (2) The SCO transition temperature $T_{1/2}$ of the PF_6 (**1**), ClO_4 (**2**), and BF_4 (**3**) salts are $T_\downarrow$ = 151.8 K, $T_\uparrow$ = 155.3 K; $T_\downarrow$ = 184.5 K, $T_\uparrow$ = 186.0 K; and $T_\downarrow$ = 146.4 K, $T_\uparrow$ = 148.2 K, respectively, demonstrating that the $T_{1/2}$ values are not in accord with the anion size.

(13) (a) Renovitch, G. A.; Baker, W. A. *J. Am. Chem. Soc.* **1967**, *89*, 2074. (b) Sorai, M.; Ensling, J.; Gütlich, P. *Chem. Phys.* **1976**, *18*, 199. (c) Spiering, H.; Meissner, E.; Koppen, H.; Muller, E. W.; Gütlich, P. *Chem. Phys.* **1982**, *68*, 65.

Experimental Section

Caution! *Perchlorate salts of metal complexes are potentially explosive. Only small quantities of material should be prepared, and the samples should be handled with care.*

Materials. All reagents and solvents used in this study are commercially available from Tokyo Kasei Co. Ltd. and Wako Pure Chemical Industries Ltd. and were used without further purification.

Ligand, 2-Methylimidazol-4-yl-methylideneamino-2-ethylpyridine (HL^{Me}). To a solution of 2-aminoethylpyridine (0.366 g, 3 mmol) in 20 mL of methanol was added a solution of 2-methyl-4-formylimidazole (0.330 g, 3 mmol) in 20 mL of methanol at room temperature. The resulting solution was warmed at 50 °C under stirring for 15 min and then cooled to room temperature. The ligand solution was used for the synthesis of the Fe^{II} complexes without further purification.

$[Fe(HL^{Me})_3](PF_6)_2$ (1). To the ligand solution (3 mmol) was added a solution of $Fe^{II}Cl_2 \cdot 4H_2O$ (0.193 g, 1 mmol) in 10 mL of methanol. To the mixture was added a solution of KPF_6 (0.376 g, 2 mmol) in 20 mL of methanol. The resulting solution was stirred at room temperature for 1 h and filtered. The filtrate was kept for a few days, during which time yellow crystals precipitated. They were collected by suction filtration. Yield: 0.35 g (35%). Anal. Calcd for $[Fe(HL^{Me})_3](PF_6)_2$, $C_{36}H_{42}FeN_{12}P_2F_{12}$: C, 42.85; H, 4.40; N, 16.70. Found: C, 42.99; H, 4.18; N, 16.67.

$[Fe(HL^{Me})_3](ClO_4)_2$ (2). To the ligand solution (3 mmol) was added a solution of $Fe^{II}(ClO_4)_2 \cdot 6H_2O$ (0.362 g, 1 mmol) in 10 mL of methanol. The resulting solution was stirred at room temperature for 1 h and filtered. The filtrate was kept for a few days, during which time yellow crystals precipitated. They were collected by suction filtration. Yellow crystals, yield: 0.30 g (33%). Anal. Calcd for $[Fe(HL^{Me})_3](ClO_4)_2$, $C_{36}H_{42}FeN_{12}Cl_2O_8$: C, 48.17; H, 4.71; N, 18.73. Found: C, 48.00; H, 4.82; N, 18.62.

$[Fe(HL^{Me})_3](BF_4)_2$ (3). To the ligand solution (3 mmol) was added a solution of $Fe^{II}(BF_4)_2 \cdot 6H_2O$ (0.337 g, 1 mmol) in 10 mL of methanol. The resulting solution was stirred at room temperature for 1 h and filtered. The filtrate was kept for a few days, during which time yellow crystals precipitated. They were collected by suction filtration. Yield: 0.28 g (32%). Anal. Calcd for $[Fe(HL^{Me})_3](BF_4)_2$, $C_{36}H_{42}FeN_{12}B_2F_8$: C, 49.57; H, 4.85; N, 19.27. Found: C, 49.81; H, 4.76; N, 19.10.

Physical Measurements. Elemental C, H, and N analyses were carried out by Ms. Kikue Nishiyama at the Center for Instrumental Analysis of Kumamoto University. TGAs were performed on a TG/DTA6200 (Seiko Instrument Inc.), where the samples of ca. 3 mg for the PF_6 and BF_4 salts were heated from room temperature to 130 °C. Due to potential explosion, the measurement for the ClO_4 salt was not performed. DSC measurements were performed with a Perkin-Elmer Pyris 1. The samples were located in sealed samples pans, and the DSC profiles were recorded at a rate of 5 K min^{-1}.

Magnetic susceptibilities were measured with a Quantum Design MPMS XL5 magnetometer in the temperature range of 5−300 K at 0.5 K min^{-1} under an applied magnetic field of 0.5 T. The calibration was done with palladium metal. Corrections for diamagnetism were made using Pascal's constants.[14] The Mössbauer spectra were recorded using a Wissel 1200 spectrometer and a proportional counter. As the radioactive source, $^{57}Co(Rh)$ moving in a constant acceleration mode was used. The hyperfine parameters were obtained by least-squares fitting to Lorentzian peaks. The isomer shifts are reported relative to metallic iron foil. The sample temperature was controlled by a Heli-tran liquid transfer refrigerator (Air Products and Chemicals Inc.) with an accuracy of ±0.5 K.

Crystallographic Data Collection and Structure Analyses. The X-ray diffraction data were collected with a Rigaku RAXIS RAPID imaging plate diffractometer using graphite monochromated Mo Kα radiation (λ = 0.71073 Å) equipped with a Rigaku cooling device. The structures were solved by direct methods and expanded using the Fourier technique. Hydrogen atoms were fixed at the calculated positions and refined using a riding model. All calculations were performed using the Crystal Structure crystallographic software package.[15]

Acknowledgment. This work was in part supported by a Grant-in-Aid for Science Research (no. 16205010) from the Ministry of Education, Science, Sports, and Culture, Japan. We thank Miss. Kikue Nishiyama at the Center for Instrumental Analysis of Kumamoto University for the elemental analyses.

Supporting Information Available: Mössbauer parameters for $[Fe^{II}(HL)_3](PF_6)_2$. This material is available free of charge via the Internet at http://pubs.acs.org.

(14) Kahn, O. *Molecular Magnetism*; VCH: Weinheim, Germany, 1993.

(15) CRYSTALS Issue 10: Watkin, D. J.; Prout, C. K.; Carruthers, J. R.; Betteridge, P. W. *CRYSALIS*, version 170; Oxford-Diffraction, Chemical Crystallography Laboratory: Oxford, U. K., 2002.